EasyChair Preprint

№ 9339

Synthesis, Characterization, DNA Interactions, Cleavage, Cytotoxic Evaluation and Molecular Modeling Studies of of Tin–Based Cancer Chemotherapy Drug as Topoisomerase I Inhibitor

Waddhaah Mohammed Abdulgaleel Al-Asbahy,
Mfeed K. A. Hassan and Manal Mohammed

November 18, 2022

2nd International Conference of Technology, Science & Administration – 2021
Taiz University
23 -25 Oct, 2022, Taiz
2nd ICTSA -2022 Proceedings

Synthesis, Characterization, DNA Interactions, Cleavage, Cytotoxic evaluation and Molecular modeling studies of of Tin–based cancer chemotherapy drug as topoisomerase I inhibitor

Waddhaah M. Al–asbahy[1,*], Mfeed K. A. Hassan [2], and Manal Shamsi[3]

[1]Department of Chemistry, Faculty of Applied Science, Taiz University, Taiz, Yemen

[2] Department of Biology, Faculty of Applied Science, Taiz University, Taiz, Yemen

[3] Department of Labratories, Faculty of Medicine and Medical Sciences, Taiz University, Taiz, Yemen

Email address:
wadahm2007@yahoo.com (Waddhaah M. Al - asbahy).

[*]Corresponding author

To cite this article:
Waddhaah M. Al - asbahy.Paper Title. *ICTSA – 2021Proceedings*, 2021, pp. x-x.

Received: MM DD, 2020; **Accepted**: MM DD, 2020; **Published**:MM DD, 2021

Abstract:
The new organotin complex **1** derived from propyl gallate and 1,10–phenanthroline was designed, synthesized and characterized by spectroscopic (IR, UV–vis, ESI–MS and (^{1}H, ^{13}C, ^{119}Sn) NMR and elemental analytical methods. the underlying mechanisms of the anticancer action of complex **1** was further elucidated by evaluating its *in vitro* DNA interaction studies of complex **1** with calf thymus DNA and the regulating signaling pathways. The *in vitro* DNA binding studies of **1** with calf thymus DNA in Tris–HCl buffer was studied by various biophysical methods (Uv/Vis, Fluorescence, and circular dichroism) which reveal that complex **1** bind to CT DNA non–covalently *via* electrostatic interaction. The higher K_b value of complex **1** suggested greater DNA binding propensity. The complex **1** exhibits DNA cleavage activity with supercoiled pBR322 in the presence of different activators. The complex cleaves DNA efficiently involving oxidative cleavage pathway. Molecular docking studies were performed to understand the binding mode of complex **1** with CT–DNA (PDB ID: 1BNA).

Keywords: Propyl gallate, 1,10–phenanthroline, *In vitro* DNA binding, topoisomerase I, pBR322 oxidative cleavage**.**

1. Introduction

Biomedical inorganic chemistry considered one of the most rapidly developing areas of pharmaceutical research for cancer therapy [1]. The discovery of truly novel metal based drugs with its mechanisms of binding with biomolecular targets are a vibrant area of research for the development of anticancer chemotherapeutic drugs [2]. Most effectiveness of chemotherapeutic anticancer drugs are compounds that interact with DNA directly through changing of the replication of DNA and inhibiting the growth of the tumor cells [3]. There are mainly three binding modes when a metal based drug binds to DNA: the electrostatic binding, the groove binding and the intercalation binding. The effect of the drug correlates closely to the selectivity of it to the AT, GC base-pairs or particular sequences [4]. The binding affinity could enhance the local concentration of the metal complex around DNA and consequently the cleavage activity. The higher propensities of complexes for DNA binding, followed by DNA cleavage are the prerequisites for a drug to act as an antitumor agent [5]. The Tin(IV) and organotin(IV) complexes exhibited an effective DNA cleavage activity both in the absence and presence of different activators at physiologically relevant conditions.

Propyl gallate (PG, 3,4,5-trihydroxybenzoic acid propyl ester) as a synthetic antioxidant exerts a variety of effects on tissue and cells due to low toxicity of PG [6]. Several studies demonstrate the benefits of PG as an antioxidant and anti-inflammatory agent. Moreover, The

protective effects of PG against oxidative DNA damage were evaluated by formation of 8-oxoguanine as a marker [7]. PG has a proven chemotherapeutic effect on HeLa and human leukemia cells due to inhibits the growth of HeLa and human leukemia cells by depleting intracellular glutathione (GSH) levels and changes the redox characteristics of HeLa cells by increasing the production of reactive oxygen species (ROS) and the activities of superoxide dismutase (SOD) and catalase. The GSH depletion-mediated apoptosis and ROS production induced by PG in HeLa cells. Generally, anticancer effects of PG was to evaluate through helpful of PG in treated of human cell lines , *viz*., human acute myeloid leukemia cell lines, THP-1 and HL-60 cells, and one human T cell lymphoblast-like cell line, Jurkat cells [8].

Tin(IV) and organotin(IV) complexes show high *in vitro* antitumor activity and in vivo anti proliferative activity. Tin(IV) complexes has some properties such as increased water solubility, lower general toxicity and fewer side effects than platinum drugs [9]. Tin complexes are well-known for promising pharmacological profile. In fact that tin based complexes exhibit cytotoxic activity against different human tumor cell lines [10]. Tin(IV) based complexes prefer to bind to the oxygen atom of the phosphate of the poly-anionic structure of DNA . Tin(IV) ions possess a hard Lewis acid nature, neutralize the negative charge of the phosphate moiety of the DNA backbone and thus brings conformational changes in DNA. The Tin(IV) and organotin(IV) scaffolds display novelty due to the dual mode of action at the molecular level [11,12].

Metal complexes of 1,10-phenanthroline (phen) are particularly attractive because they can effectively bind to DNA in different modes of interaction. The major pathway for DNA damage by 1,10-phenanthroline in the complexes is believed to involve C10-hydrogen atom abstraction, along with varying amounts of oxidation at the C40- and/or C50-positions in DNA [13].

In this paper, we report the synthesis, spectroscopic characterization and *in vitro* DNA binding studies of an organotin(IV) complex. We also demonstrate the *in vitro* antitumor activity of the tin complex. We have carried out *in vitro* interaction studies of tin(IV) complex with multiple drug targets, *viz*. DNA and topoisomerase I inhibition, which revealed its potential to act as an intercalating DNA binding agent which mediates its anticancer activity *via* inhibition of the topoisomerase I activity. Moreover, molecular docking studies have been employed to explore the orientation, specific binding sites and non–covalent interaction of tin(IV) complex within the binding cavity of targeted biological macromolecule (DNA and topoisomerase I).

2. Materials & Methods

2.1. Reagents and materials

All reagents were of the best commercial grade and were used without further purification. $(CH_3)_2SnCl_2$ (Sigma–Aldrich), Propyl gallate (Fisher Scientific), 1,10 phenathrolein (Loba chemie). All of the antibodies used in this study were purchased from Cell Signaling Technology (Beverly, MA). Tris(hydroxymethyl)aminomethane or Tris Buffer (Sigma), 6X loading dye (Fermental Life Science) and Super coiled plasmid DNA pBR322 (Genei) were utilized as received. Disodium salt of calf thymus (CT DNA) DNA was purchased from Sigma. Chemical Company was stored at 4 °C. Doubly distilled water was used as the solvent throughout the experiments.

2.2. Methods and Instrumentation

Carbon, hydrogen and nitrogen contents were determined using Carlo Erba Analyzer Model 1108. Molar conductance was performed at room temperature on a Digisun Electronic conductivity Bridge. Fourier–transform IR (FTIR) spectra were recorded on an Interspec 2020 FTIR spectrometer. Electronic spectra were recorded on UV–1700 PharmaSpec Uv–vis spectrophotometer (Shimadzu). Data were reported in λ_{max}/nm. Interaction of complex with calf thymus DNA was performed in 0.01 M buffer (pH 7.2). Solutions of calf thymus DNA in buffer gave a ratio of absorbance at 260 nm and 280 nm of ca 1.9 indicating that DNA was free from protein. Cleavage experiments were performed with the help of Axygen electrophoresis supported by Genei power supply with a potential range of 50–500 Volts, visualized and photographed by Vilber–INFINITY gel documentation system.

2.2.1. DNA–binding and cleavage experiments

DNA binding experiments include absorption spectral traces, emission spectroscopy and circular dichroism conformed to the standard methods and practices previously adopted by our laboratory [14]. While measuring the absorption spectra an equal amount of DNA was added to the compound solution and the reference solution to eliminate the absorbance of the CT DNA itself, and the CD contribution by the CT DNA and Tris buffer was subtracted through base line correction. The cleavage experiments of supercoiled pBR322 DNA (300 ng) by complex **1** (10–30 μM) in Tris–HCl/NaCl (5:50 mM) buffer at pH 7.2 was carried out using agarose gel electrophoresis. The samples were incubated for 45 min at 310 K. A loading buffer containing 25% bromophenol blue, 0.25% xylene cyanol, 30% glycerol was added and electrophoresis was carried out at 50 V for 1 h in Tris–HCl buffer using 1% agarose gel containing 1.0 mg/ml ethidium bromide. The DNA cleavage with added reductant was monitored as in case of cleavage experiment without added reductant using agarose gel electrophoresis.

2.2.2. Topoisomerase I inhibition assay

DNA topoisomerase I, Human (Topo–I) was purchased from CALBIOCHEM and was used without further purification. One unit of the enzyme was defined as completely relaxed 1 μg of negatively supercoiled pBR322 DNA in 30 min at 310 K under the standard assay conditions. The reaction mixture (30 μL) contained 35 mM Tris–HCl (pH 8.0), 72 mM KCl, 5

mM MgCl2, 5 mM DTT, 2 mM spermidine, 0.1 mg mL^{-1} BSA, 0.25 µg pBR322 DNA, 2 Unit Topo I and Sn(IV) complex. These reaction mixtures were incubated at 310 K for 30 min, and the reaction was terminated by addition of 4 µL of 5× buffer solution consisting of 0.25% bromophenol blue, 4.5% SDS and 45% glycerol. The samples were electrophoresed through 1% agarose in TBE at 30 V for 8 h**.**

2.2.3. Statistical and synergy analysis

All experiments were carried out at least in triplicate and results were expressed as mean ± S.D. Statistical analysis was performed using SPSS statistical program version 13 (SPSS Inc., Chicago, IL). Difference between two groups was analyzed by two–tailed Student's t–test. Difference with P <0.05(*) or P <0.01(**) was considered statistically significant. The difference between three or more groups was analyzed by was analyzed by one–way ANOVA multiple comparisons.

2.2.4. Molecular docking studies

The rigid molecular docking studies were performed by using HEX 6.8 software, [15] is an interactive molecular graphics program for calculating and displaying feasible docking modes of a pairs of protein, enzymes and DNA molecule. The coordinates of metal complex was taken from its crystal structure as a CIF file and was converted to the PDB format using Mercury software. The crystal structure of the B–DNA dodecamer $d(CGCGAATTCGCG)_2$ (PDB ID: 1BNA was downloaded from the protein data bank (http://www.rcsb.org./pdb). All calculations were carried out on an Intel pentium4, 2.4 GHz based machine running MS Windows XP SP2 as operating system. Visualization of the docked pose have been done by using CHIMERA (http://www.cgl.ucsf.edu/chimera/) and PyMol (http://pymol.sourceforget.net/) molecular graphics program.

2.2.5. Synthesis of $C_{12}H_{14}N_2Cl_2Sn$ (1)

This complex was prepared in a manner analogous to that of complex **1**, using $(CH_3)_2SnCl_2$ (0.219 g, 1 mmol) in place of $(CH_3)_2SnCl_2$ (Figure 1). A white coloured precipitate was obtained, which is filtered, washed with cold MeOH and dried under vacuo over anhydrous $CaCl_2$. Yield = 46%. M.P. ≥ 230 ± 2°C. Anal. Calc. for $C_{12}H_{14}N_2Cl_2Sn$ (%) C, 42.05; H, 5.53; N, 7.01, Found: C, 41.99; H, 5.67; N, 7.09. Λ_M(1.00×10^{-3} M, DMSO): 32.55 $\Omega^{-1}cm^2$ mol^{-1} (non-electrolyte). IR (KBr, cm^{-1}): 3400 ν(O–H), 1621 (C=N), 1586 ν_{as}(COO),1510 (δOCH_2, δCH_2 , δCCH_3), 1468 (C–N), 678 (Sn–O), 416 (Sn–N), 642 (Sn–C). ^{1}H NMR (400 MHz, DMSO, δ): 0.99(–CH_3), 2.50 (–CH_2–), 3.33 (C–CH_2–), 4.15 (HO–), 7.16 (protons of aromatic moeity), 8.02–8.75 (protons of phen ligand), 7.99 (–N=CH–). ^{13}C NMR (100 MHz, DMSO, δ): 9.30(–CH_3), 40.17 and 23.99(–CH_2–CH_2–),168.22 (C=N), 123– 144 (aromatic carbons), 149.33 (C–O), 175.0 (C=O). ^{119}Sn NMR (149.12 MHz, DMSO, δ): –363.47. Uv-vis absorption: λ_{max} (DMSO, 10^{-3} M), nm (ε/10^3 M^{-1} cm^{-1}) 266 (1.23), 281 (0.66) and 311 (0.36). ESI-MS (m/z): 404.1

3. Results & discussion

3.1. Chemistry

Complex **1** is stable in air and soluble in dimethylsulfoxide (DMSO) solvent. An outline of the synthetic procedure of the ligand and its tin complex is presented in Figure 1. The coordination geometry of central metal ion Sn(IV) atom was present in hexacoordinated environment, which was proposed on the basis of spectroscopic studies (IR, Uv–vis, ^{1}H, ^{13}C, ^{119}Sn NMR, ESI-MS) and elemental analytical data. The results obtained through these techniques are in agreement with the proposed 1:1:1 stoichiometry between the Sn(IV) moieties and ligands. The in vitro binding studies of **1** with CT DNA were carried out by using absorption, emission spectroscopic titrations and gel electrophoresis.

3.2. Spectral characterization

In the IR spectrum of the propyl gallate-based ligand exhibited broad band of ν(O–H) in the range of 3200–3500 cm^{-1}. The characteristic envelop at around 3400 cm^{-1} merged and broadened due to the complexation [16]. Also, The individual assignment of each –OH group was difficult as both the –OH groups are known to absorb in the same region. The IR spectra of the complex **1** displayed peaks at 1535, 1586 and 1882 cm^{-1} which were assigned to –(C=O) vibrations. The bands appearing between 1468 and 1510 cm^{-1} were attributed to (δOCH_2, δCH_2 , δCCH_3) for the propyl gallate moiety in the all complexes.

Additionally, in the complex **1** absorption bands at 642–678 cm^{-1} for ν(Sn–O) were observed which correspond to deprotonation of phenolic OH due to coordination with central tin(IV) atom. The coordination of 1,10-phenanthroline molecule to Sn(IV) ions was supported by the appearance of medium intensity band in the region 416–444 cm^{-1} attributed to ν(Sn–N). In the IR spectrum of the complex **1** a medium intensity band at 539 and 507 cm^{-1}, respectively, corresponds to ν(Sn–C) [17].

The electronic spectrum of complex **1** in DMSO displayed three strong bands at ca. 266, 278 and 311 nm, in the ultra–violet (UV) region, attributed to intraligand transitions. The absorption spectrum of complex **1** was also investigated at different times (24, 36 and 72 hours), neither precipitation nor any change in the spectroscopic pattern was observed, which confirm the stability of complex 1 in solution.

The complex **1** was characterized by ^{1}H NMR spectroscopy. The spectra exhibited characteristic signals of the asymmetric –CH_2–O,–CH_2– and –CH_3 protons in the vicinity of 3.3, 2.5 and 0.99 ppm, respectively. The aromatic proton of propyl gallate signatures were observed in the range of 7.86–6.78 ppm. While in complex **1**, the presence of Sn–Ph protons at range 7.16–7.52 ppm. In the ^{1}H NMR spectra of the complex **1**, the H(8) of 1,10-phenanthroline molecule appears at 8.02–9.32 ppm [16].

^{13}C NMR spectrum of the complex **1** exhibited the strong characteristic signal of (C=O) at 175–178 ppm, the coordination of tin(IV) to nitrogen atom was observed in the spectra at 165–168 ppm. The six aromatic carbon peaks appeared in the range 144–123 ppm [19]. The carbons of the

($-CH_2CH_2CH_3$) moiety appeared in the range 48.73–9.30 ppm [20].

The validation of the geometry of tin(IV) metal ion in **1** was done by ^{119}Sn NMR spectroscopy. It is known that ^{119}Sn chemical shiftd (^{119}Sn) is sensitive towards the coordination sphere around the tin atom. ^{119} Sn NMR showed a single peak at –363.47 ppm, –253.53 and –572.38 ppm for complex **1** confirming the octahedral geometry around the tin atoms in complex **1** [21].

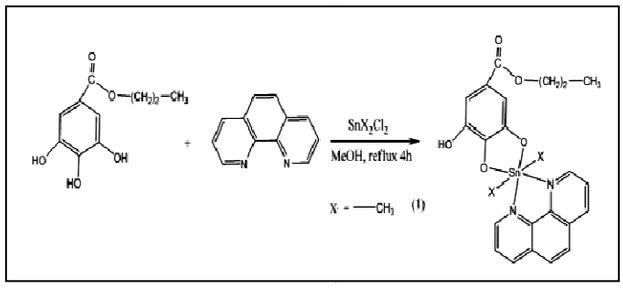

Figure 1. *Synthetic route for complex **1**.*

3.2. DNA binding studies

3.2. 1. DNA binding studies

The absorption spectra of **1** in the absence and presence of CT–DNA at constant concentration of complexes are shown in Figure 2. The complex **1** exhibited intraligand absorption bands in the UV region at 266, 280 and 311–325 nm, respectively, assigned to (π–π*) and LMCT transitions, respectively. On addition of CT-DNA (increasing concentration (0.033–2.00)×10^{-4} M) to complex **1**, there is a sharp hyperchromic effect in the absorption bands due to electrostatic binding mode and stabilization of the complex–DNA adduct. Moreover, hyperchromic effect reflects the corresponding changes of DNA in its conformation and structure after the complex–DNA interaction has taken place. The Sn(IV) ions (non transition metal ion) of the complexes exhibit preferential selectivity towards the phosphate group of the DNA backbone which lead to contraction and conformational change of DNA helix. However, the presence of Propyl gallate in a drug is caused to degradation of CT–DNA through oxidative DNA damage pathway [22].

To evaluate quantitatively, the binding strengths of **1** with CT DNA, the intrinsic binding constants K_b of the complexes were determined with Eq. (1) by monitoring the changes in absorbance bands with increasing concentration of CT DNA [23]:

$$\frac{[DNA]}{[\varepsilon_a-\varepsilon_f]}=\frac{[DNA]}{[\varepsilon_b-\varepsilon_f]}+\frac{1}{K_b[\varepsilon_b-\varepsilon_f]} \quad (1)$$

and ε_b are the apparent extinction coefficient $A_{obs}/[M]$, the extinction coefficient for free metal complex and the extinction coefficient for metal complex in the fully bound form, respectively. In the plots of [DNA]/ε_a –ε_f versus [DNA], K_b is given by the ratio of the slope to the intercept.

The binding constant obtained for **1** is 3.50×10^4 M^{-1}. The K_b values revealed that **1** exhibits stronger binding affinity towards CT DNA.

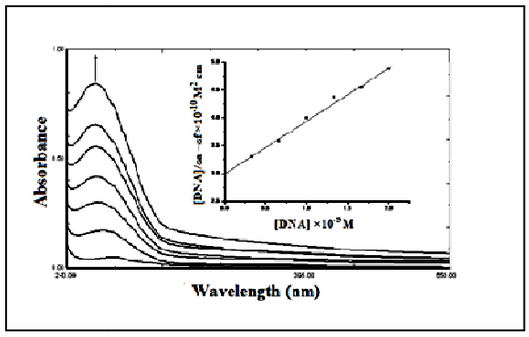

Figure. 2. *Variation of UV–vis absorption of complex **1** with increase in the concentration of CT DNA in buffer 5mM Tris–HCl/50 mM NaCl, pH=7.2 at 25 °C. Inset: plots of [DNA]/ εa -εf versus [DNA].*

3.2. 2. Fluorescence interaction studies

At room temperature, the complex **1** emit strong luminescence in Tris–HCl buffer with a maximum wavelength of 364 nm when excited at 266 nm. Fixed amounts of **1** (1.00×10^{-5} M) were titrated with increasing amounts of DNA (0.033–2.00)×10^{-5}M). Titration of CT-DNA led to a remarkable decrease in the emission intensity of **1**, as shown in Figure 3, respectively. Complex **1** produced a large decreased in emission intensity in the presence of DNA. The quenching behavior of the luminescent excited state of the complex was due to electron and energy transfer from the phenanthroline based emission state to the base pairs and inducing the decrease of emission intensity [24].

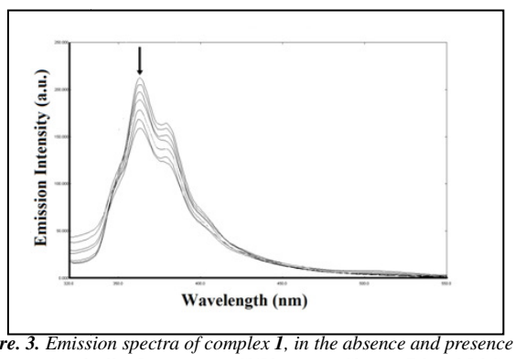

Figure. 3. *Emission spectra of complex **1**, in the absence and presence of CT DNA in buffer 5mM Tris–HCl/50 mM NaCl, pH=7.2 at 25 °C.*

3.2.3. Circular dichroism study

Circular dichroism spectroscopy is useful in diagnosing changes in DNA morphology during drug–DNA interactions. The band due to base stacking (~275 nm) and that due to right–handed helicity (~245 nm) are quite sensitive to the mode of DNA interactions with small molecules. Simple groove binding and electrostatic interaction of the complex **1** with DNA shows less or no perturbation on both the bands while intercalator enhances the intensities of both bands. The

CD spectra of complex **1** on addition of CT DNA showed strong conformational changes by the complexes, the intensity of negative band decreased (shifted to zero level), while the positive band increased with slightly changes in the wavelength and maximum increase of ellipticity was observed indicating stronger DNA binding (Figure 4). This phenomenon could be due to groove binding that stabilizes the right–handed B–form of DNA [25].

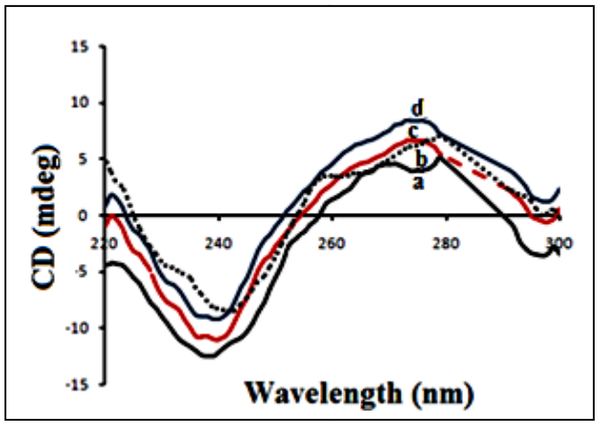

Figure 4. *CD spectrum of (a) CT-DNA alone (b,c, and d) CT-DNA in presence of* ***1*** *at different concentrations.*

3.2.4. DNA cleavage assay

The cleavage reaction can be monitored by gel electrophoresis. When circular plasmid DNA is conducted by electrophoresis, the fastest migration will be observed for the supercoiled form (Form I). If one strand is cleaved, the supercoils will relax to produce a slower–moving nicked circular form (Form II). If both strands are cleaved, a linear form (Form III) that migrates between Form I and Form II will be generated [26]. Figure 5 shows agarose gel electrophoresis patterns of pBR322 DNA after incubation with of complex **1** for 45 mins in Tris–HCl buffer (pH 7.2) at 37ºC. Compared with DNA control (Lane 1), the conversion of supercoiled form (form I) to nicked form (form II) becomes more efficient with increasing concentration of complex **1** reached to 40 µM, the linear form III was manifested in the gel (lane 5), and the percentage of linear DNA increases with the increase of the concentration of complex **1**. So, it is clear that cleavage of pBR322 DNA is highly dependent on metal ions concentration.

The nuclease activity of the complex has been The DNA cleavage activity of complex **1** was also evaluated in presence of different activators, *viz*., H_2O_2, 3–mercaptopropionic acid (MPA), glutathione (GSH) and ascorbic acid, the cleavage pattern is depicted in Fig. 7. The cleavage activity of **1** was significantly enhanced by these activators and follows the order H_2O_2>MPA >GSH>Asc for **1**.

Reactive oxygen species (ROS) generated during the interaction between metal complexes and dioxygen or redox reagents are responsible for the DNA cleavage catalyzed by the metal complexes [27]. reactions were carried out in the presence of typical scavengers such as hydroxyl radical scavengers (DMSO, tert–butyl alcohol), singlet oxygen quencher (NaN_3) and superoxide scavenger (SOD) under our experimental conditions [28]. As shown in Figure 6, which indicated that the tert–butyl alcohol (lane 7) and NaN_3 (lane 8) diminished the DNA breakdown by complex **1**, which indicates that the hydroxyl radical and singlet oxygen scavenger participates in the oxidative DNA cleavage. DMSO (lane 6) had no significant effect on the DNA cleavage, also addition of superoxide dismutase (superoxide scavenger) to the reaction mixture did not show any appreciable inhibitory effect on the chemical nuclease activity by the complex **1** (Lane 9). From these results, we can conclude that a complex **1** species, singlet oxygen $^1O_2$ and hydroxyl radical $^{\bullet}OH$ are the active species involved in the DNA strand scission. Hence, the cleavage pattern thus observed supported the oxidative *cleavage pathway.*

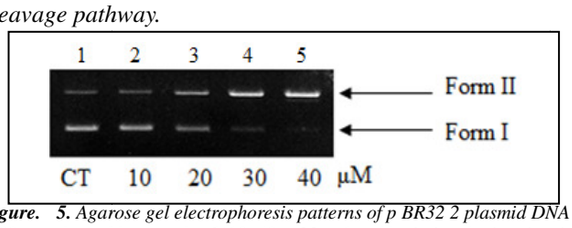

Figure. 5. *Agarose gel electrophoresis patterns of p BR32 2 plasmid DNA (300 ng) cleaved by complex* ***1****(10–40 m M), after 45 min incubation time in buffer (5mM Tris–HCl/50 mM NaCl, pH=7.2 at 25 °C) (concentration dependent).*

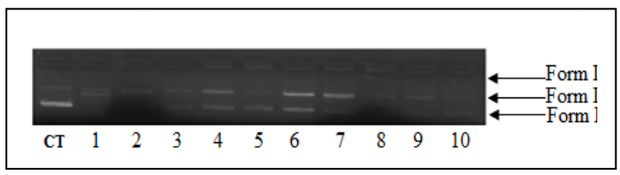

Figure. 6. *Agarose gel electrophoresis pattern for the cleavage pattern of pBR322 plasmid DNA (300 ng) by complex* ***2*** *(0.25 mmol) in the presence of different activating agents at 37 ◦ C after incubation for 45 min: Lane 1, DNA control; Lane 2, DNA +* ***1*** *+H_2O_2 (0.4 M); Lane 3, DNA +* ***1*** *+ MPA (0.4 M); Lane 4, DNA +* ***1*** *+ GSH (0.4 M); Lane 5, DNA +* ***1*** *+ Asc (0.4 M); Lane 6, DNA +* ***1*** *+ DMSO (0.4 M); Lane 7, DNA +* ***1*** *+ tert-butyl alcohol (0.4 M); Lane 8, DNA +* ***1*** *+ NaN_3 (0.4 M); Lane 9, DNA +****1*** *+ Superoxide Dismutase (15 units). Lane 10, DNA +* ***1*** *+ Methyl green (2.5 L of a 0.01 mg/mL solution); Lane 11, DNA +* ***1*** *+ DAPI (8 M)*

3.2.5. Topoisomerase I inhibition.

A plasmid DNA cleavage assay was used to investigate the effect of Sn(IV) complex on the activity of human Topo–I by agarose gel electrophoresis. This assay provides a direct means of determining whether the drug affects the unwinding of a supercoiled (SC) duplex DNA to nicked open circular (NOC) and relaxed (R) DNA. When the catalytic activity of topoisomerase I was assayed, complex **1** inhibited this process in a concentration dependent manner [29]. As shown in Figure 7, supercoiled DNA was fully relaxed by the enzyme in the absence of tin complex (lane 2, Topo–I). However, upon increasing the concentration of tin complex (5–10 µM), the levels of relaxed form were inhibited (lanes 3–5). At 8.12 µM the DNA relaxation effect caused by Topo–I was completely inhibited by Sn(IV) complex. These observations suggest that Sn(IV) complex inhibits topoisomerase I catalytic activity due to the relatively strong DNA binding affinity of Sn(IV) complex, which prevents the enzyme from efficiently binding to the DNA. Thus, the tin–based drug entity can exert its antitumor activity *via* topoisomerase I inhibition.

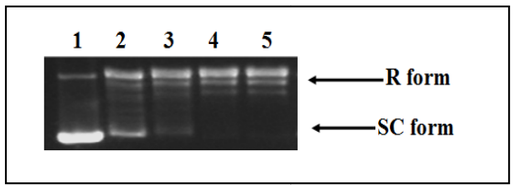

Figure 7. *Agarose gel electrophoresis patterns showing the effect of different concentrations of Sn (IV) complex on the activity of DNA topoisomerase I (Topo–I); lane 1, DNA control; lane 2, Topo–I + DNA; lane 3, 5 μM of Sn(IV) complex + DNA + Topo–I; lane 4: 7.5 μM of Sn(IV) complex + DNA + Topo–I; lane 5: 10 μM of Sn(IV) complex + DNA + Topo–I.*

3.2.6. Molecular docking studies with DNA

After satisfactory spectroscopic measurement of DNA binding study of the complex **1**, molecular docking study was performed to understand the Drug–DNA interactions in rational drug design, as well as in the mechanistic study by placing a small molecule into the binding site of the target specific region of the DNA mainly in a non–covalent fashion [30]. In our experiment, rigid molecular docking (two interacting molecules were treated as rigid bodies) studies was performed to predict the binding modes of complex **1** with DNA duplex of sequence d(CGCGAATTCGCG)$_2$ dodecamer (PDB ID:1BNA) provide an energetically favorable docked pose that is shown in Figure 8. The result shows that complex **1** interacts with DNA *via* electrostatic mode involving outside edge stacking interactions with the oxygen atom of the phosphate backbone of DNA. In this model, it is clearly indicated that complex **1** fits snugly into the curved contour of the targeted DNA in the minor groove and is situated within G–C rich region thus, leads to van der Waals interaction and hydrophobic contacts with DNA functional groups that define the groove [31]. Moreover, the propyl gallate moiety of the complex **1** arranged in a parallel fashion with respect to the deoxyribose groove walls of the DNA was stabilized by hydrogen bonding (~3.9 Å) between –OH of propyl gallate with N3 and anomeric oxygen of deoxyribose of A6A and O2 of C21B with –N=CH group of 1,10–phenanthroline ligand. The resulting relative binding energy of docked metal complex **1** with DNA was found to be –202 KJ mol^{-1}. Thus, molecular docking study together with spectroscopic studies, which can be provide valuable information about the mode of interaction of the complex with DNA and the conformation constraints for adduct formation.

4. Conclusion

Organotin(IV) complex **1** of propyl gallate and 1,10–phenanthroline was synthesized and thoroughly characterized. *In vitro* DNA binding studies of the complex **1** employing UV–Vis titrations, fluorescence, circular dichroism and gel electrophoresis were carried out to ascertain the mode of binding and the extent of binding. The results supported the fact that complex **1** bind to CT DNA via electrostatic mode of interaction as well as selective binding to the minor groove of DNA. The complex **1** cleaves supercoiled plasmid DNA through an oxidative (O_2–pathway) cleavage mechanism induced by a reactive oxygen species (ROS).

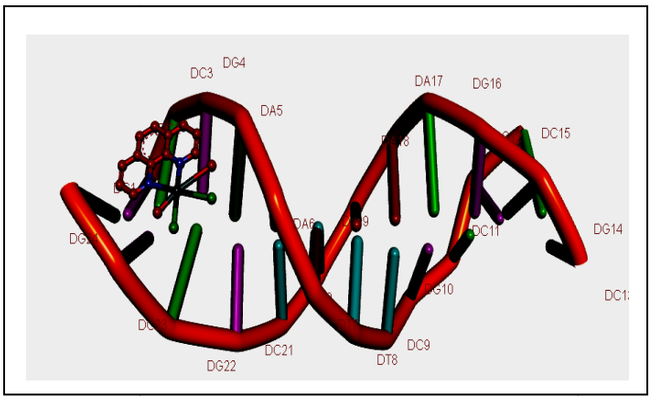

Figure 8. *Molecular docked model of Sn(IV) complex with DNA dodecamer duplex of sequence d(CGCGAATTCGCG)2 (PDB ID: 1BNA).*

Furthermore, In Sn(IV) complex exhibits significant anti–proliferative activity indicative of apoptosis, Sn(IV) complex exhibits significant inhibitory effects on Topo–I activity at a very low concentration,~8.12 μM. Molecular docking studies was performed with molecular target DNA in order to validate the experimental results. Therfore, The present study highlights the importance of the tin(IV) complex **1**, which has potential to serve as a potent antitumor agent by interacting with the biological target DNA at the molecular level.

5. References

[1] Cancer Research UK, UK Cancer Incidence Statistics byAge, /http://info. cancerresearchuk.org/cancerstats/incidence/age/S, (January2007), Retrieved 2007-06-25.

[2] Casini, J. Exploring the mechanisms of metal–based pharmacological agents via an integrated approach. J. Inorg. Biochem. 2012, 109,97–106.

[3] Mary, C. W.; Dawn, M. H.; Jennifer, E. B.; Lucy, A. P.; Melissa, G.; Jane, H. S. Age and Cancer Risk. Am. J. Prev. Med. 2014, 46, S7–15.

[4] Catherine, M.; Damien, G.; Freddie, B.; Jacques, F.; Gary, M. C. Global burden of cancer attributable to infections in 2018: a worldwide incidence analysis. Lancet. Glob. Health. 2020, 8(2),e180–e190.

[5] DeVita, V. T.; Lawrence, T. S.; Rosenberg, S. A. Cancer Principles & Practice of Oncology. Wolters Kluwer. 2019, 11th edition.

[6] Tobias, J.; Hochhauser, D. Cancer and its management (7th edition). Wiley Blackwell. 2015.

[7] Shaloam, D.; Paul, B. T. Cisplatin in cancer therapy: molecular mechanisms of action. Eur. J. Pharmacol. 2014, 740, 364–378.

[8] Xue, X.; Matthew, D. H.; Qiang, Z.; Paul, C. W.; Michael, M. G.; Xing–Jie, L. Nanoscale Drug Delivery Platforms Overcome Platinum–Based Resistance in Cancer Cells Due to Abnormal Membrane Protein Trafficking. ACS Nano. 2013, 7(12), 10452–10464.

[9] Sotiris, H.; Nick, N. H. Antiproliferative and anti–tumor activity of organotin compounds. Coord. Chem. Rev. 2009, 253, 235–249.

[10] Pengpeng, J.; Ruizhuo, O.; Penghui, C.; Xiao, T.; Xia, Z.; Tian, L. Review: recent advances and future development of metal complexes as anticancer agents. J. Coord. Chem. 2017, 70, 2175–2201.

[11] Waddhaah, M. A.; Sabah, A. A.; Manal, Shamsi.; Tianfeng C. Design, synthesis and characterization of tin–based cancer chemotherapy drug entity: In vitro DNA binding, cleavage, induction of cancer cell apoptosis by triggering DNA damage–mediated p53 phosphorylation and molecular docking. Appl. Organometal. Chem. 2018, e4651, 1–14.
[12] Huzaifa, Y. K.; Santosh, K. M.; Hifzur, R. S. Shariq, Y.; Farukh, A. New Tailored RNA–Targeted Organometallic Drug Candidates against Huh7 (Liver) and Du145 (Prostate) Cancer Cell Lines, ACS Omega. 2020, 5, 25, 15218–15228
[13] Susanta, H.; Anup, P.; Gunjan, S.; Armando, P. Sulfonated Schiff Base Sn(IV) complexes as potential anticancer agents. J. Inorg. Biochem. 2016, 162, 83–95.
[14] Waddhaah, M. A.; Mohammad, U., Farukh, A.; Manal, S.; Sartaj, T. A dinuclear copper(II) complex with piperazine bridge ligand as a potential anticancer agent: DFT computation and biological evaluation. Inorganica Chimica Acta. 2016, 445, 167–178.
[15] Diana, M.; David, W. R. Docking essential dynamics eigenstructures. Proteins. 2005, 60, 269–274.
[16] Nicolas, P. E. B.; Peter, J. S. Exploration of the medical periodic table: towards new targets. Chem. Commun. 2013, 49, 5106–5131.
[17] Marcel, G.; Tin–based antitumour drugs. Coord. Chem. Rev. 1996, 151, 41–51.
[18] Sartaj , T.; Waddhaah, A.; Mohd, A.; Vivek, B. Molecular drug design, synthesis and structure elucidation of a new specific target peptide based metallo drug for cancer chemotherapy as topoisomerase I inhibitor. Dalton Transactions. 2012,41(16),4955–4964.
[19] Anayive, P–R.; De Lima, G.M.; Marchini, N.; Beraldo, H. structural studies and cytotoxic of N(4)–phenyl–2–benzoylpyridine thiosemicarbazone Sn(IV) complexes. Eur. J. Med. Chem. 2005, 40, 467–472.
[20] Bhaskar, C.; Elangovan, N.; Sowrirajan, S.; Chandrasekar, S.; Ola, A. A.; Samy, F.M.; Renjith, T. Synthesis, XRD, Hirshfeld surface analysis, DFT studies, cytotoxicity and anticancer activity of di(m–chlorobenzyl) (dichloro) (4, 7–diphenyl–1,10–phenanthroline) tin (IV) complex. J. Molecular Structure. 2022, 1267, 133542.
[21] Latha, A.; Elangovan, N.; Manoj, K.P.; Keerthi, M.; Balasubramani, K.; Sowrirajan, S.; Chandrasekar, S.; Renjith, T. Synthesis, XRD, spectral, structural, quantum mechanical and anticancer studies of di(p–chlorobenzyl) (dibromo) (1, 10–phenanthroline) tin (IV) complex. J. Ind. Chem. Soc. 2022, 99(7), 100540.
[22] Burl, Y.; Sean, P.; David, A. A. Synthesis and characterization of organotin Schiff base chelates. Inorg. Chim. Acta. 2002, 333, 124–131.
[23] Attila, J.; László, N.; Erlend, M.; Einar, S. Potentiometric and spectroscopic evidence for co–ordination of dimethyltin(IV) to phosphate groups of DNA fragments and related ligands. J. Chem. Soc., Dalton Trans. 1999, 1587–1594.
[24] Friedman, A. E ; Kumar, C. V.; Turro, N. J.; Barton, J. K. Luminescence of ruthenium(II) polypyridyls: evidence for intercalative binding to Z–DNA. Nucleic Acids Res. 1991, 19, 2595–2602.
[25] Jacqueline, K.B.; Avis, D.; Jonathan, G. Tris(phenanthroline)ruthenium(II): stereoselectivity in binding to DNA. J. Am. Chem. Soc. 1984, 106, 2172–2176.
[26] Charles, A. D.; Filomena, V. P.; Jeffrey, R. Bocarsly. Molecular Recognition Effects in Metal Complex Mediated Double–Strand Cleavage of DNA: Reactivity and Binding Studies with Model Substrates. Inorg. Chem. 1997, 36, 17, 3676–3682.
[27] Trotta, E., Del Grosso, N., Erba, M., and Paci, M. The ATT strand of AAT.ATT trinucleotide repeats adopts stable hairpin structures induced by minor groove binding ligands. Biochemistry. 2000, 39(23), 6799–6808.
[28] Dong–Dong, L.; Jin–Lei, T.; Wen, G.; Xin, L.; Shi–Ping, Y. DNA binding, oxidative DNA cleavage, cytotoxicity, and apoptosis–inducing activity of copper(II) complexes with 1,4–tpbd (N,N,N′,N′–tetrakis(2–yridylmethyl)benzene–1,4–diamine) ligand. J. Inorg. Biochem. 2011, 105, 894–901.
[29] Beatriz, M.; Wilmar, C.; Marc, M.; Rupert, Ö.; Joan, A. DNA Interaction and Dual Topoisomerase I and II Inhibition Properties of the Anti–Tumor Drug Prodigiosin. Toxicol. Sci., 2005, 85, 870–879.
[30] Rohs,R.; Bloch, I.; Sklenar, H.; Shakked, Z. Molecular flexibility in ab initio drug docking to DNA: binding–site and binding–mode transitions in all–atom Monte Carlo simulations. Nucleic Acids Res. 2005, 33 (22), 7048–7057.
[31] Rosanna, F.; Antonella, P.; Simone, D.;, Paolo, de C.; Giuseppe, B. Molecular modelling studies, synthesis and biological activity of a series of novel bisnaphthalimides and their development as new DNA topoisomerase II inhibitors. Bioorg. Med. Chem. 2009, 17, 13–24.

Acknowledgements

We are thankful to Regional Sophisticated Analytical Instrumentation Facility, Panjab University, Chandigarh, India for providing ESI-MS and running the ^{1}H, ^{13}C, and ^{31}P NMR, Sophisticated Test and Instrumentation Centre, Cochin University, Cochin, India for providing elemental analysis and Finally, we are extremely grateful to Dr. Rizwan Hasan Khan, Interdisciplinary Biotechnology Unit, Aligarh Muslim University, for CD facility.